NIRT: Bio-Nano-Robotic Systems Using Viral Protein Nano-Motors

NSF NIRT Grant DMI – 0303950 and DMI-0422724
PI: Mavroidis C.[1]; co-PIs: Yarmush M.[2,3], Papadimitrakopoulos F.[4], Tomassone S.[5]
[1]Department of Mechanical & Industrial Engineering, Northeastern University, Boston, MA
[2]Department of Biomedical Engineering, Rutgers University, Piscataway, NJ
[3]Center for Engineering in Medicine, Massachusetts General Hospital, Boston, MA
[4]Department of Chemistry, University of Connecticut, Storrs, CT
[5]Department of Chemical & Biochemical Engineering, Rutgers University, Piscataway, NJ

Overview: The recent explosion of research in nano-technology, combined with important discoveries in molecular biology has created a new interest in biomolecular machines and robots. The main goal in the field of biomolecular machines is to use various biological elements — whose function at the cellular level creates a motion, force or a signal — as machine components that perform the same function in response to the same biological stimuli but in an artificial setting [1, 2]. In this way proteins and DNA could act as motors, mechanical joints, transmission elements, or sensors. If all these different components were assembled together they could potentially form nanodevices with multiple degrees of freedom, able to apply forces and manipulate objects in the nanoscale world, transfer information from the nano- to the macroscale world and even travel in a nanoscale environment. In this project, we are studying the development of Viral Protein Linear (VPL) nano-motors and their integration as actuators in bio-nano-robotic systems. The project consists of three research phases: 1) Performance of computational studies to develop models and design procedures that will predict and optimize the performance of the proposed bio-nano motors and systems; 2) Execution of experimental studies to demonstrate the validity of the proposed concepts, models and design methodologies; and 3) Establishment of the interface of the proposed protein motors with other biomolecular components such as DNA joints and carbon-nanotube rigid links so that complex, multi-degree of freedom machines and robots powered by the VPL motors are formed. In this overview we present the current activities and results in all research phases.

Principle of Operation: In order to infect new cells, several viruses employ proteins on their surface that undergo changes in their structural conformation in order to promote the fusion of the viral membrane with the cellular membrane. This change is due to the pH change associated with the vicinity of the cell. Given similar conditions, it is proposed in this project to use this conformational change to produce VPL motors. In the first year of this project we have focused our computational and experimental studies in the influenza virus and its hemagglutinin protein. As the pH of the viral containing vesicle drops, the hemagglutinin protein undergoes a dramatic conformational change, which promotes the placement of fusion peptides into the cellular membrane. It has been shown that this conformational change can be described as a spring-like mechanism, where the hemagglutinin protein is originally folded into a meso-stable state, with a hinge-like motif. Upon a change in the pH, the hinge-like region irreversibly extends into a α-helical fold, which puts the hemagglutinin protein into a more stable low-energy conformation. The hinge-like region has previously been isolated and studied, and it has been shown that it is able to undergo a reversible transition from a disordered peptide at a pH of 7.0 to a stable α-helix upon a change in pH to 4.8 at low temperatures [3]. The sequence for the hinge-like region has been identified as a 36 amino acid peptide called *loop36*. During the first year of this project we have focused our studies on the *loop36* that has a closed length of about 4 nm and an extended length of about 6 nm, giving it an extension by two thirds of its length.

Computational Studies: The computational work consisted of the development of algorithms and programs to perform the molecular dynamic and kinematic simulations of the proposed Viral Protein Lineal (VPL) Nano-motors. To predict and characterize the dynamic performance of the proposed VPL motors (i.e. energy and force calculation) we performed Molecular Dynamic (MD) Simulations that are based on the calculation of the free energy that is released during the transition from native to fusogenic state. We used the MD software called CHARMm (Chemistry at Harvard Molecular Mechanics). *Loop36* peptides were modeled individually as well as

trimers. The effect of pH was simulated by protonating 10 titrable amino acids (Glutamic Acid - GLU, Aspartic Acid - ASP, and Histidine - HIS). MD simulations ranging from 10 ps to 1 ns were performed before and after protonation of HIS, ASP and GLU. The peptides were also mutated by replacing GLY22 by ALA (G22A) in line with the experimental observations. Targeted Molecular Dynamics (TMD) and Steered Molecular Dynamic (SMD) simulations were also performed to design hybrid simulations that will lead to the desired conformations and will follow a feasible trajectory. We can then calculate the forces, velocities and displacements in order to characterize the motor. Molecular kinematic simulations have also been developed to study the geometric properties and conformational space of the VPL motors. The kinematic analysis was based on the development of direct and inverse kinematic models and their use towards the workspace analysis of the VPL motors. An example simulation is shown in Figure 1 where a *loop36* monomer was pulled apart in SMD and subjected to MD with and without protonation in order to see the effect of protonation. Additional information on our computational studies on the VPL nanomotors can be found in [4] and in http://www.bionano.neu.edu

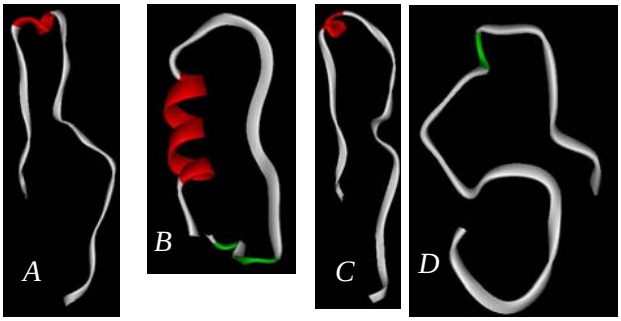

Figure 1: Unprotonated *Loop36* monomer pulled by SMD (A) when subjected to MD simulations regains its helical character and comes back to a state similar to the crystal structure (B) defined state at high pH. *Loop36* monomer does not revert back to its stable conformation with partial alpha-helical character (C) when protonated (D).

Table 1: Site-directed mutations of *loop 36*

Position in Peptide	Native Amino Acid	Mutated Amino Acid
4	Glutamate (E)	Glutamine (Q)
8	Glutamate (E)	Glutamine (Q)
11	Histidine (H)	Glutamine (Q)
14	Glutamate (E)	Glutamine (Q)
16	Glutamate (E)	Glutamine (Q)
19	Glutamate (E)	Glutamine (Q)
21	Glutamate (E)	Glutamine (Q)
22	Glycine (G)	Alanine (A)
28	Glutamate (E)	Glutamine (Q)
32	Glutamate (E)	Glutamine (Q)

Experimental Studies: Our efforts thus far have focused substantially on the mutagenesis, expression, purification, and characterization of *loop36*. We have cloned, mutagenized, purified and characterized *loop36*, and 10 genetically engineered mutants (Table 1) by circular dichroism (CD) spectroscopy. Our results raise interesting questions about the purported ability of wild-type *loop36* to undergo a complete structural transition, while suggesting alternative approaches that substantially improve the pH-responsiveness of the wild-type peptide. Table 1 shows the mutants that were produced for this study. After

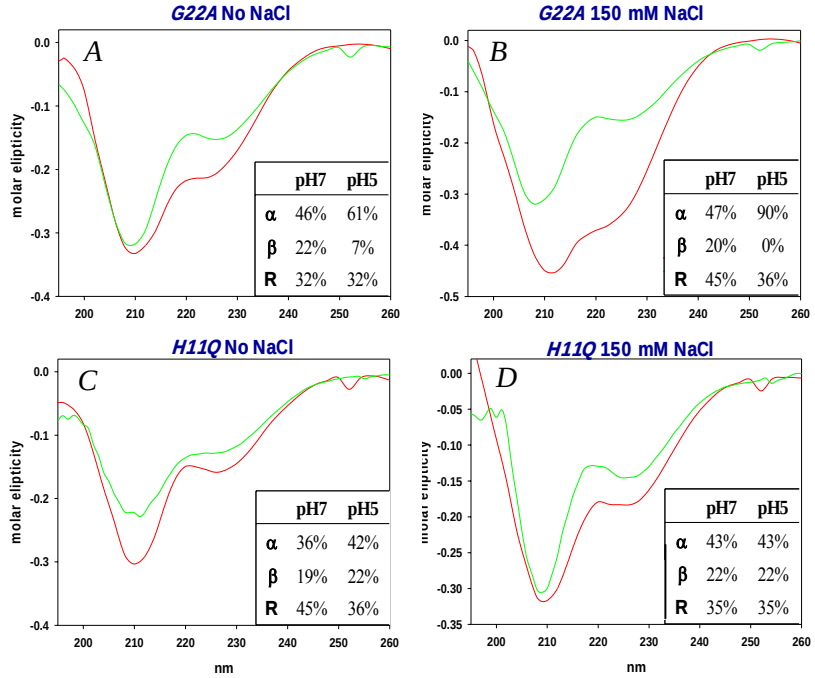

Figure 2: *A-B.* The G22A mutant exhibits an increased α-helical content at lower pH. This transition, which is more pronounced in the presence of 150 mM NaCl, comes at the expense of β-sheet structure and random coils. *C-D.* The H11Q mutant exhibits a slight increase in α-helicity and β-sheet conformation, at lower pH, in the absence of NaCl, but not in its presence.

an initial screen, for improvement in the random coil to α-helix transition, we focused our efforts on the characterization of the wild-type (*wt*), glycine-alanine mutation at position 22 (*G22A*), and histidine to glutamine mutation at position 11 (*H11Q*). In contrast to the results of Carr and Kim [3], we did not observe a significant increase in the α-helical content of *wt loop36* when changing the pH from 7 to 5. Carr and Kim (1993) reported a high random coil content at pH 7 and a high α-helical content at pH 5 (more than 99% in each case). By contrast, our wild-type *loop36* contained approximately 31% α-helical content at both pHs. After characterizing the mutants listed in Table 1, we found two mutants with improved random coil to α-helix transitions, in comparison to the *wt*. Mutants *G22A* and *H11Q* both exhibited an increase in α-helical content in response to a decrease in pH (Figure 2).

Interface of VPL with Other Components: Our initial efforts are concentrated into developing a polymerizable bilayer membrane matrix, where the VPL could be organized and aligned perpendicular to the matrix. The development of these polymerizable bilayer membrane matrices were also geared to provide additional visualization ability to these coil-to-helix transition. This was based on chromism of the diacetylene backbone that has been recently attracted considerable attention for bio-sensor applications. Such system could prove particularly useful in observing the coil-to-helix transition expected for the VPL during pH changes. Assuming that we are capable of incorporating VPL moieties within a diacetylene-based bilayer membrane, the coil-to-helix transition is expected to generate significant volume change which should be accompanied by profound changes in their absorption spectra. This, however, implies that changes of pH should result in negligible variation in the UV-Vis absorption spectra of these polymerized bilayer membrane matrices. For this purpose, our laboratory has synthesized three diacetylenic surfactants shown in Figure 3. The terminal group of these surfactants is based on the non-ionizable hydroxyl- or ethylene oxide-unit which enables adequate water affinity, yet should remain unaffected over large pH variation. A variety of synthetic routes were utilized to synthesize the above compounds. Following their synthesis, the molecular structures and purity were verified with ^{1}H NMR, GC-Mass and melting point analysis. Liposomes of these amphiphiles were prepared using ultra-sonication and polymerized by exposing them to UV light (254 nm) for 5 to 10 min. On the basis of UV-Vis changes, only the PCO and PCAO were prone to polymerization. While maintaining compression, these monolayers were exposed to UV irradiation of 254 nm to polymerize their structure. PCAO exhibited the best polymerizability among the three surfactants. The resulting monolayer on water subphase was transferred onto the hydrophobic 2 by 0.7 cm^2 quartz substrate to investigate its chromaticity dependence upon pH. Figure 4 depicts UV-Vis absorbance of polymerized PCAO monolayer on quartz substrate immersed in aqueous solutions with pH of 7 and 4, respectively. The lack of significant changes upon pH illustrates this surfactant is suitable for further investigations with VPL nanomotors.

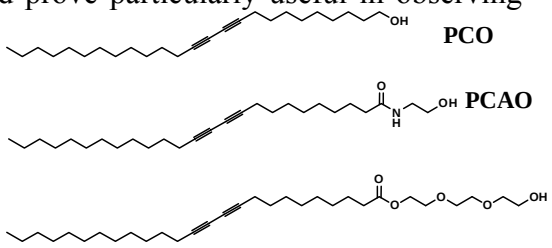

Figure 3: Chemical structures of the investigated diacetylene-based surfactants.

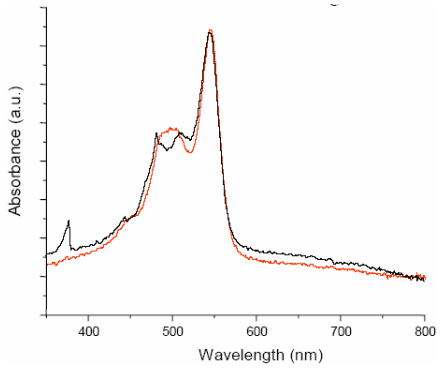

Figure 4: UV spectra of PCAO polymerized monolayer at pH 7 (black line), pH 4 (red line)

References

1. Mavroidis C. and Dubey A., "From Pulses to Motors", *Nature Materials*, Vol. 2, No 9, pp. 573-574, 2003.
2. Mavroidis C., Dubey A., and Yarmush M., "Molecular Machines", *Annual Reviews of Biomedical Engineering*, Vol. 6, 2004.
3. Carr, C.M. and Kim, P.S., 1993. "A Spring-Loaded Mechanism for the Conformational Change of Influenza Hemagglutinin", *Cell*, 73(4): 823-32.
4. Dubey A., Sharma G., Mavroidis C., Tomassone S. M., Nikitczuk K.P., Yarmush M.L., "Computational Studies of Viral Protein Nano-Actuators," *Journal of Computational and Theoretical Nanoscience*, Vol. 1, No. 1, pp. 18-28, 2004.